Supporting Information

A nitrogen-doped mesoporous carbon containing an embedded network of carbon nanotubes as a highly efficient catalyst for the oxygen reduction reaction

Jin-Cheng Li,[#] Shi-Yong Zhao,[#] Peng-Xiang Hou,* Ruo-Pian Fang, Chang Liu,* Ji Liang, Jian Luan, Xu-Yi Shan and Hui-Ming Cheng

Shenyang National Laboratory for Materials Science, Institute of Metal Research, Chinese Academy of Sciences, 72 Wenhua Road, Shenyang 110016, China.

E-mail: cliu@imr.ac.cn and pxhou@imr.ac.cn

[#]These authors contributed equally to this work.

1 Experimental section

1.1 Carbon nanotube (CNT) growth

0.2 g $Fe(NO_3)_3 \cdot 9H_2O$ was added to 50 ml ethanol and sonicated for dissolution. 2.0 g of a porous silica support (~7 nm in average particle size and BET surface area of 390±40 m^2/g, Sigma Aldrich) was then added to this solution. After drying the mixture using a rotary evaporator, a faint yellow powder was obtained for use as the catalyst for CNT growth.

For the growth of CNTs, ~0.5 g of the powder was placed in a quartz boat which was placed at the center of a 50-mm-diameter quartz tube in a horizontal tube furnace. The furnace temperature was raised from room temperature to 800 ^oC at a rate of 20 ^oC/min under the protection of a 1000 standard cubic centimeter per minute (sccm) Ar flow. The catalyst was then reduced for 20 min under a 1000 sccm H_2 flow. The H_2 supply was then turned off and 1000 sccm Ar, 50 sccm Ar bubbled through an ethanol tank, and 200 sccm C_2H_4 were

introduced into the furnace for CNT growth. After 150 min, the furnace was cooled naturally under the protection of an Ar flow.

1.2 Synthesis of CNT/(N-C)-X (X=700, 800 or 900)

1.0 g aniline (C_6H_7N) monomer was dissolved in 12 ml 1.0 M hydrochloric acid (HCl) followed by the addition of 20 ml 1M HCl containing 1.0 g CNTs/SiO_2. After stirring for 15 min, 5 ml of 1M HCl containing 3.0 g ammonium peroxydisulphate (APS) was added drop-wise with vigorous stirring. The polymerization was conducted in an ice bath while stirring for 24 h. After drying the mixture using a rotary evaporator, the obtained CNT-SiO_2/PANI composite was pyrolysed under 50 sccm NH_3 and 150 sccm Ar mixed gas flow at 800 ^oC for 1 h. Finally, the silica and unstable species were etched away by washing with a mixture of HF solution and concentrated HCl (3/1 vol ratio) at 70 ^oC for 12 h to obtain the CNT/(N-C)-800 catalyst. Samples CNT/(N-C)-700 and CNT/(N-C)-900 were obtained by changing the pyrolysis temperature to 700°C and 900°C, respectively.

1.3 Synthesis of no-Fe, no-MP, and no-CNT samples for the comparison study

To study the role of residual Fe in the catalysts, we synthesized a reference sample with Fe thoroughly removed (denoted no-Fe) by washing in concentrated HCl at 70 ^oC for 12 h before the aniline polymerization process. The other preparation conditions were the same as for the CNT/(N-C)-800 catalyst.

To study the role of mesopores, we synthesized a nitrogen-doped carbon with embedded CNTs that contained no mesopores (denoted no-MP) by removing the SiO_2 support before the aniline polymerization process (washed in 4 M KOH at 70 ^oC for 12 h). The other conditions were the same as for the CNT/(N-C)-800 catalyst.

To study the role of CNTs, we synthesized nitrogen-doped porous carbon without CNTs included (denoted no-CNT) by omitting the CNT growth process. The other conditions were the same as that of CNT/(N-C)-800 catalyst.

2 Supplementary figures and tables

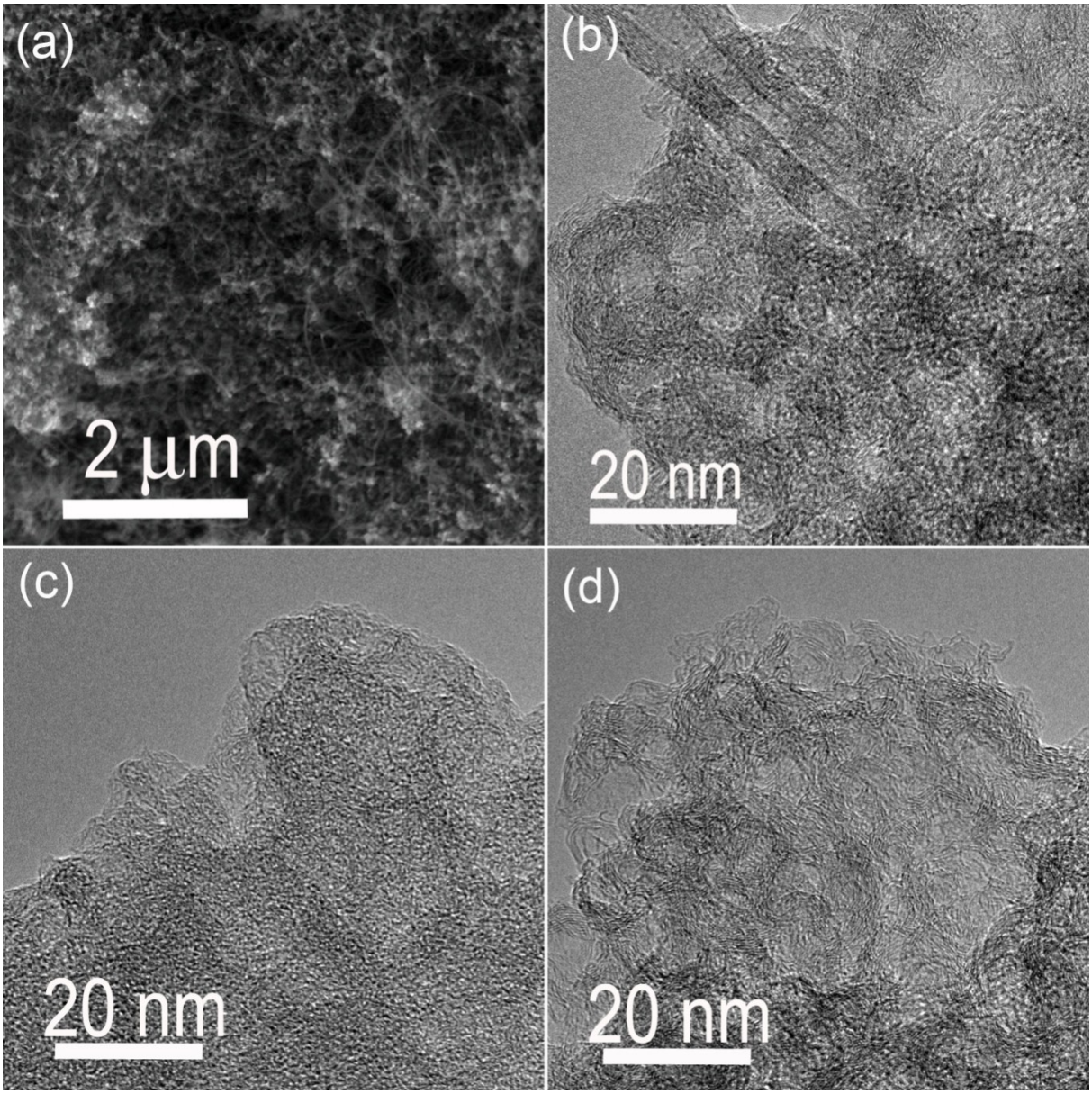

Figure S1. (a) SEM image showing that CNTs grew from the porous SiO_2 nanoparticles.

TEM images of (b) CNT/(N-C)-800, (c) CNT/(N-C)-700, and (d) CNT/(N-C)-900 catalysts.

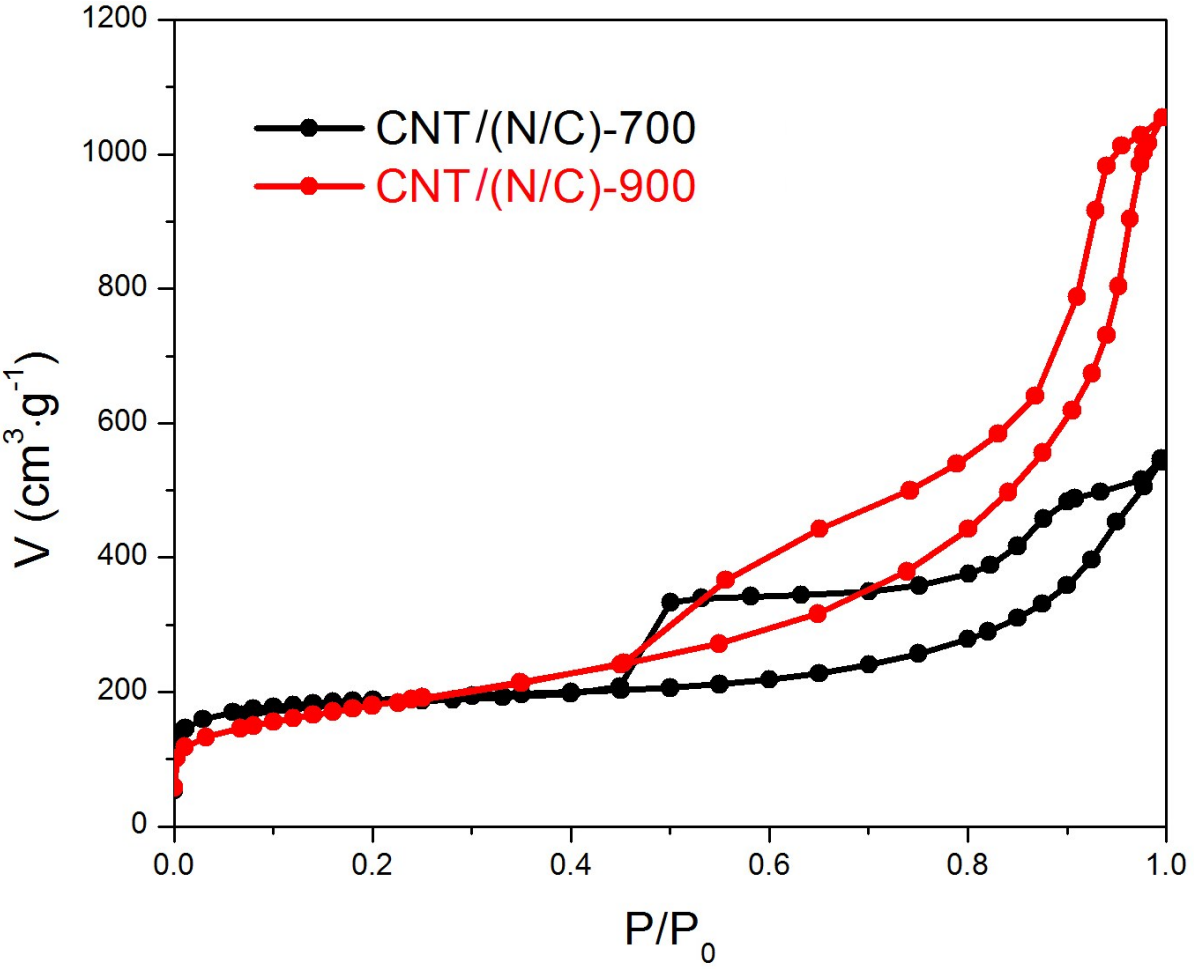

Figure S2. N_2 adsorption/desorption isotherms of the CNT/(N-C)-700 and CNT/(N-C)-900 catalysts.

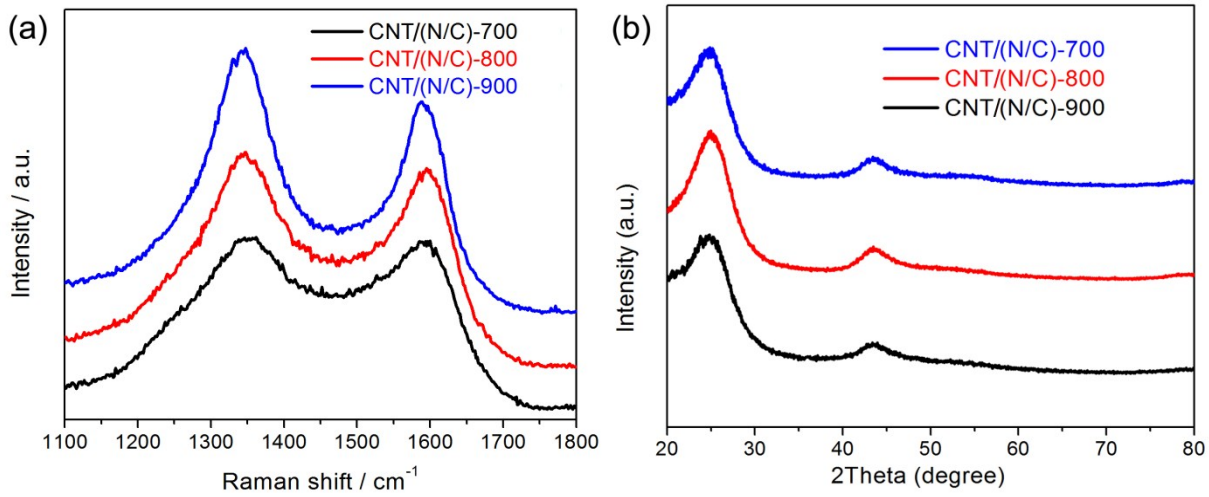

Figure S3. (a) Laser Raman spectra and (b) XRD patterns of the CNT/(N-C)-X catalysts.

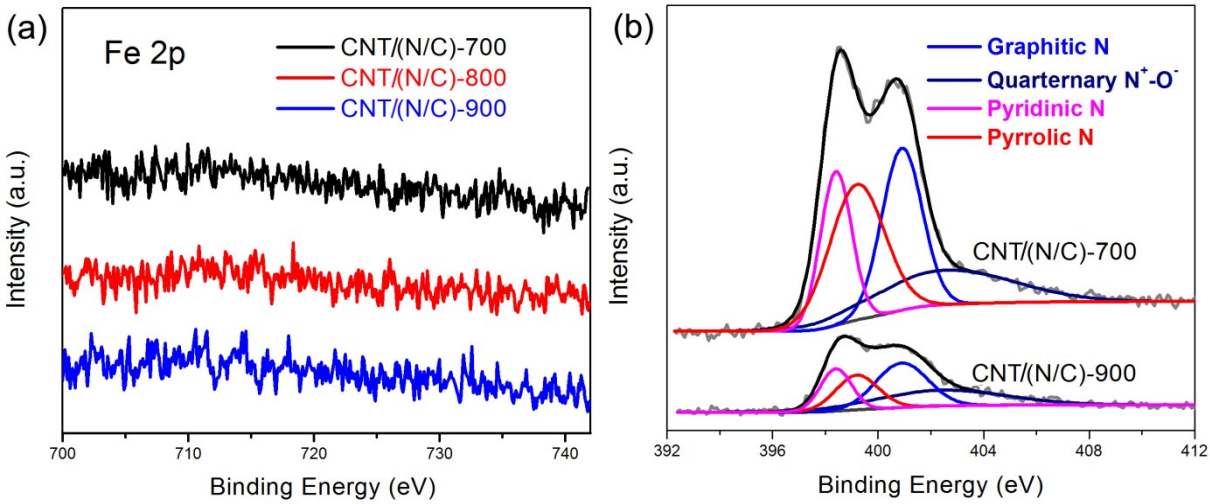

Figure S4. (a) High-resolution XPS survey scan and (b) N1s spectra of the CNT/(N-C)-X catalysts.

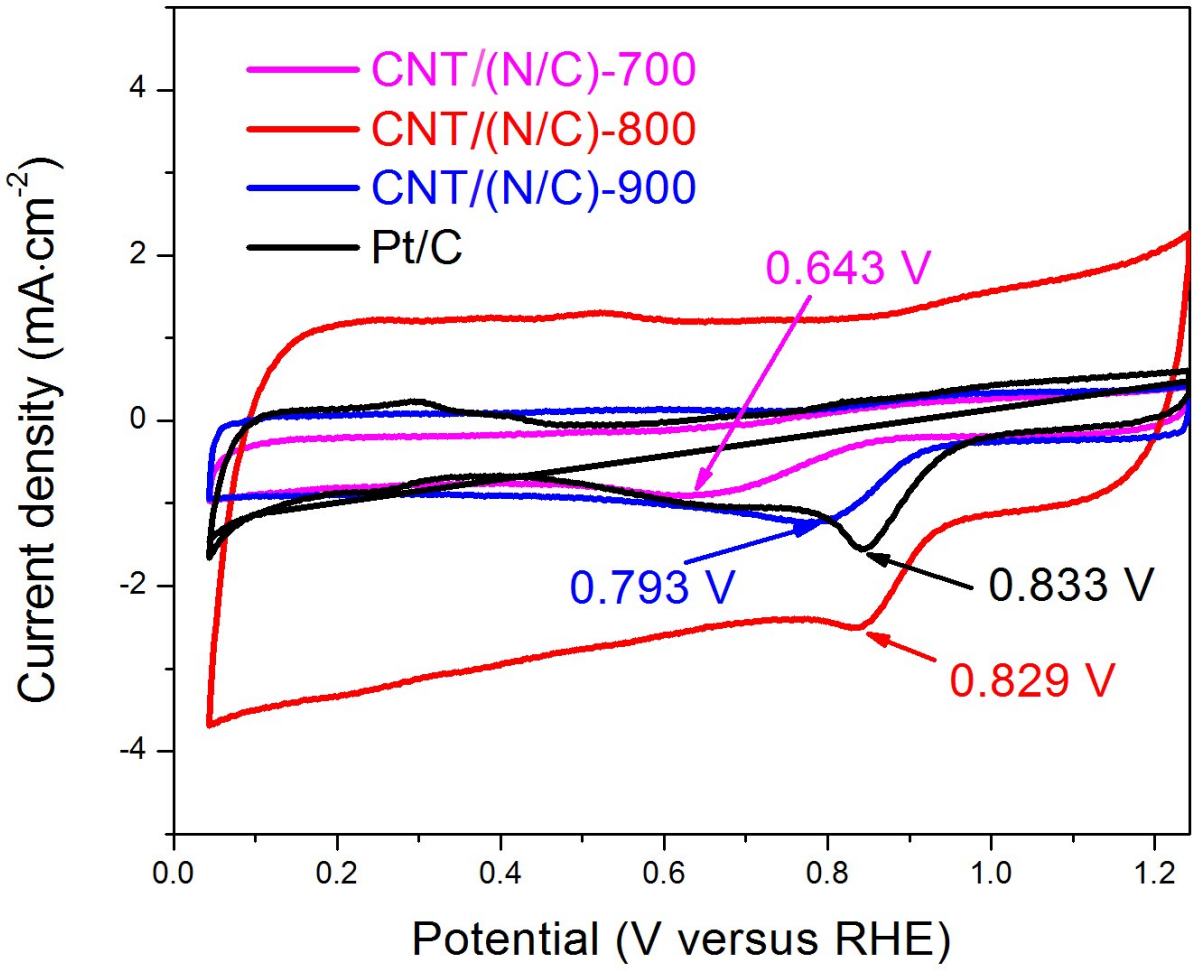

Figure S5. CV curves of the CNT/(N-C)-X catalysts measured in an O_2-saturated 0.1 M KOH solution at a scan rate of 50 mV/s.

For the calculation of the number of electrons transferred (n), we analyzed the kinetic parameters on the basis of the Koutecky–Levich equations:

$$\frac{1}{J} = \frac{1}{J_L} + \frac{1}{J_K} = \frac{1}{B\omega^{1/2}} + \frac{1}{J_K}$$

$$B = 0.62nFC_0(D_0)^{2/3}\nu^{-1/6}$$

$$J_K = \frac{1}{nkFC_0}$$

where J is the measured current density, J_K and J_L are the kinetic- and diffusion-limiting current densities, ω is the angular velocity, F is the Faraday constant ($F = 96500$ C/mol), C_0 is the bulk concentration of O_2 ($C_0 = 1.2 \times 10^{-6}$ mol/cm^3), D_0 is the diffusion coefficient of O_2 in a 0.1 M KOH solution ($D_0 = 1.9 \times 10^{-5}$ cm^2/s), ν is the kinematic viscosity of the electrolyte (ν=0.01 cm^2/s), and k is the electron-transfer rate constant. For the Tafel plot, the kinetic current was calculated from the mass-transport correction of RDE by:

$$J_K = \frac{J_L \times J}{(J_L - J)}$$

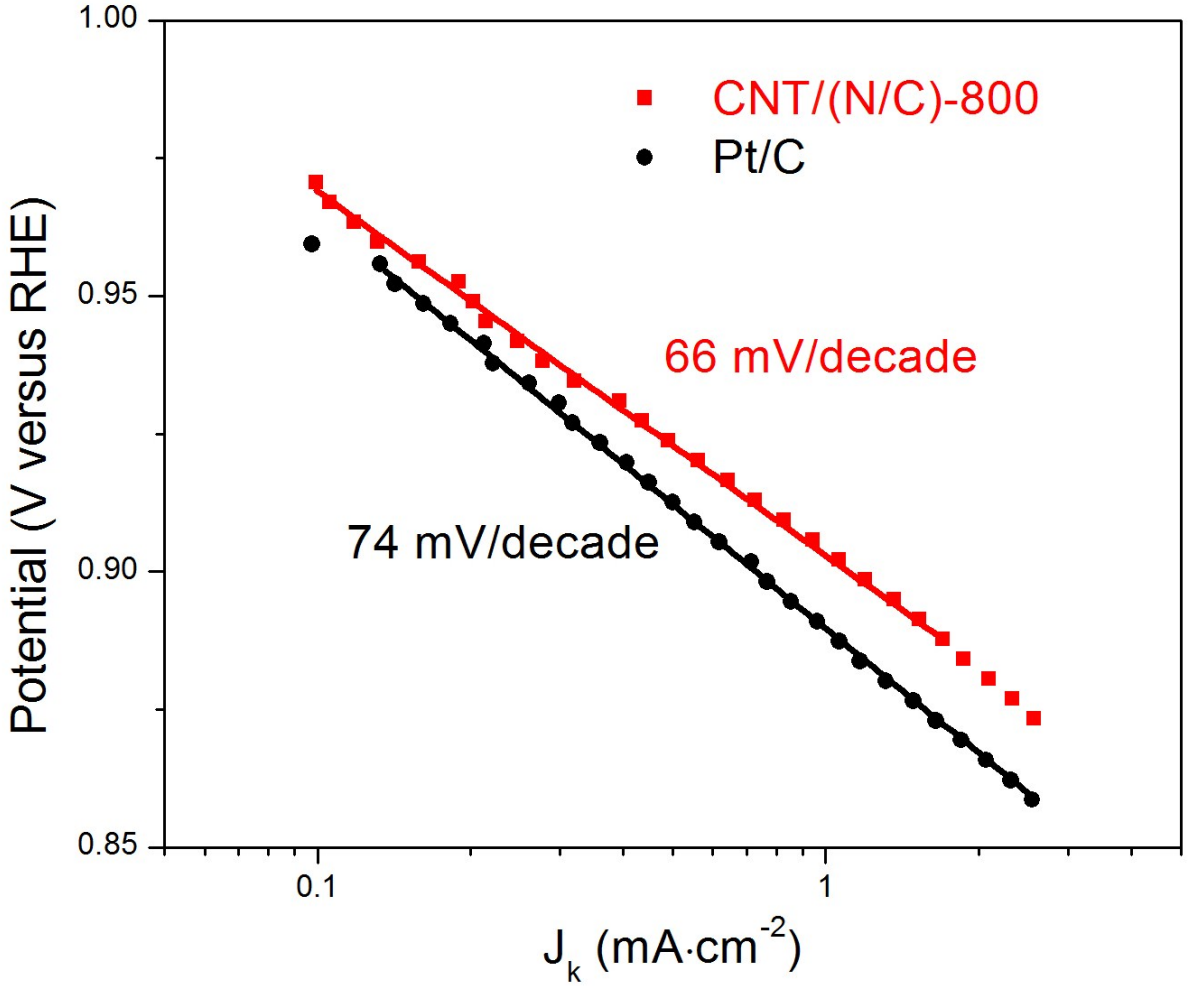

Figure S6. Tafel plot of the CNT/(N-C)-800 catalyst and a commercial Pt/C catalyst with the same loading of 0.1 mg cm^{-2}.

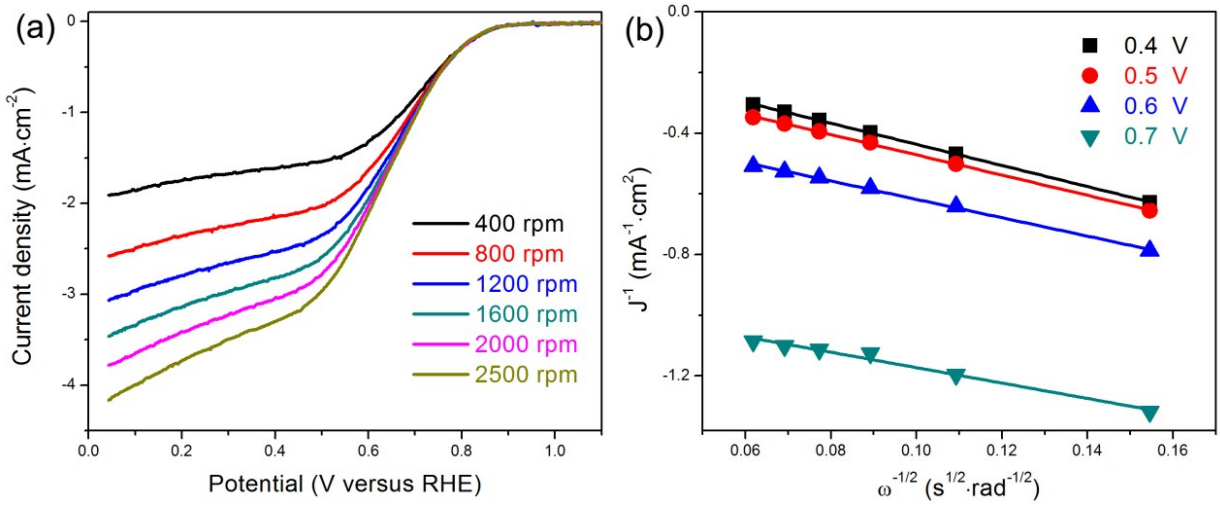

Figure S7. (a) RDE voltammograms of the CNT/(N-C)-700 catalyst at different rotation rates and (b) the corresponding Koutecky–Levich plots at 0.4, 0.5, 0.6, and 0.7 V.

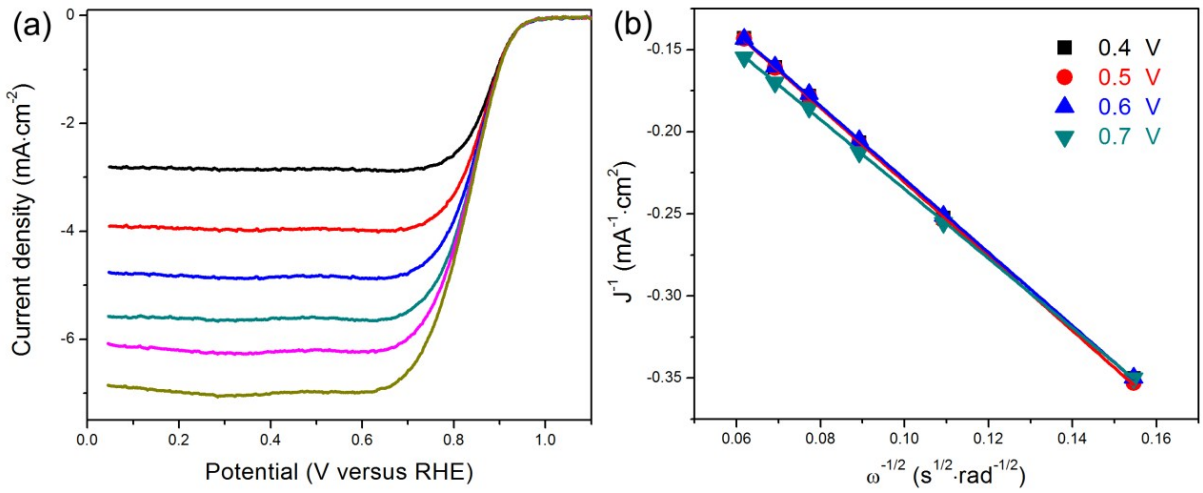

Figure S8. (a) RDE voltammograms of CNT/(N-C)-800 at different rotation rates and (b) the corresponding Koutecky–Levich plots at 0.4, 0.5, 0.6, and 0.7 V.

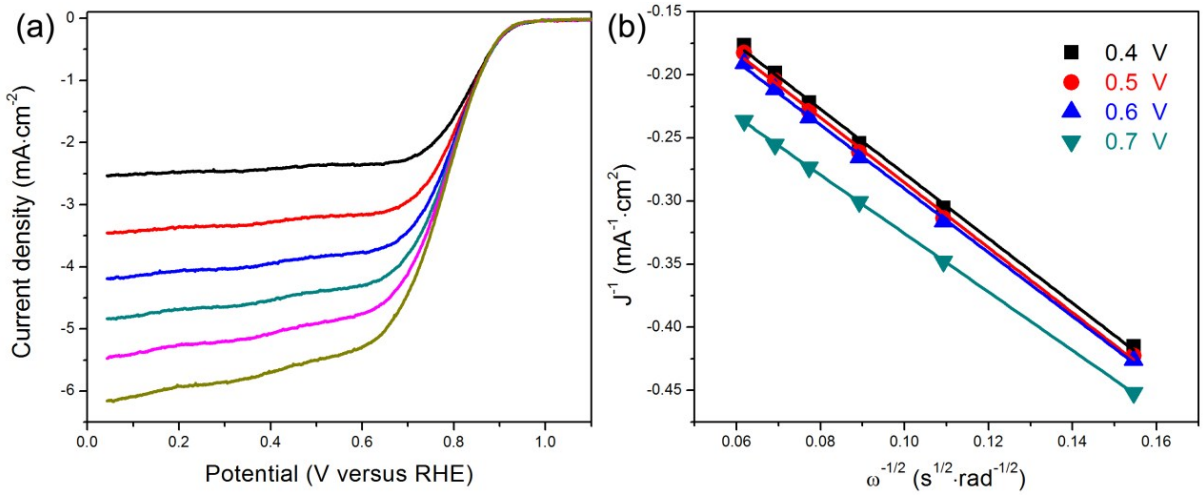

Figure S9. (a) RDE voltammograms of the CNT/(N-C)-900 catalyst at different rotation rates and (b) the corresponding Koutecky–Levich plots at 0.4, 0.5, 0.6, and 0.7 V.

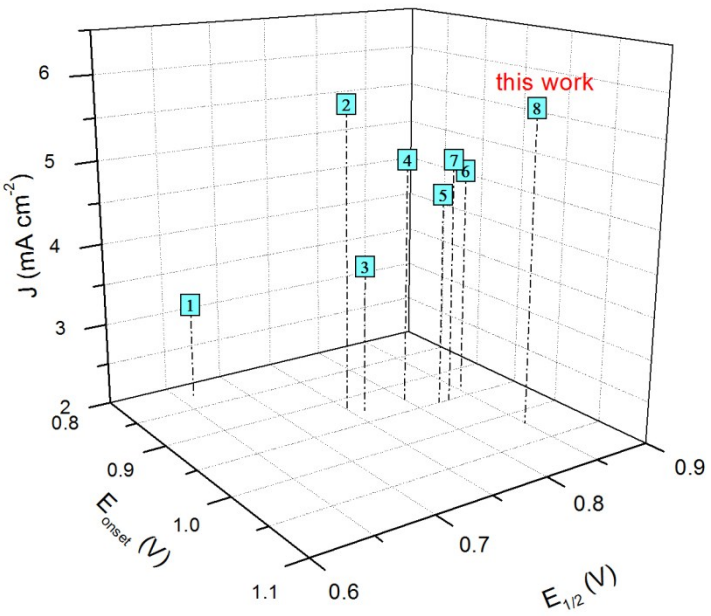

Figure S10. The ORR performance of our CNT/(N-C)-800 catalyst and that of some other N-doped carbonaceous electrocatalysts reported previously[1-7].

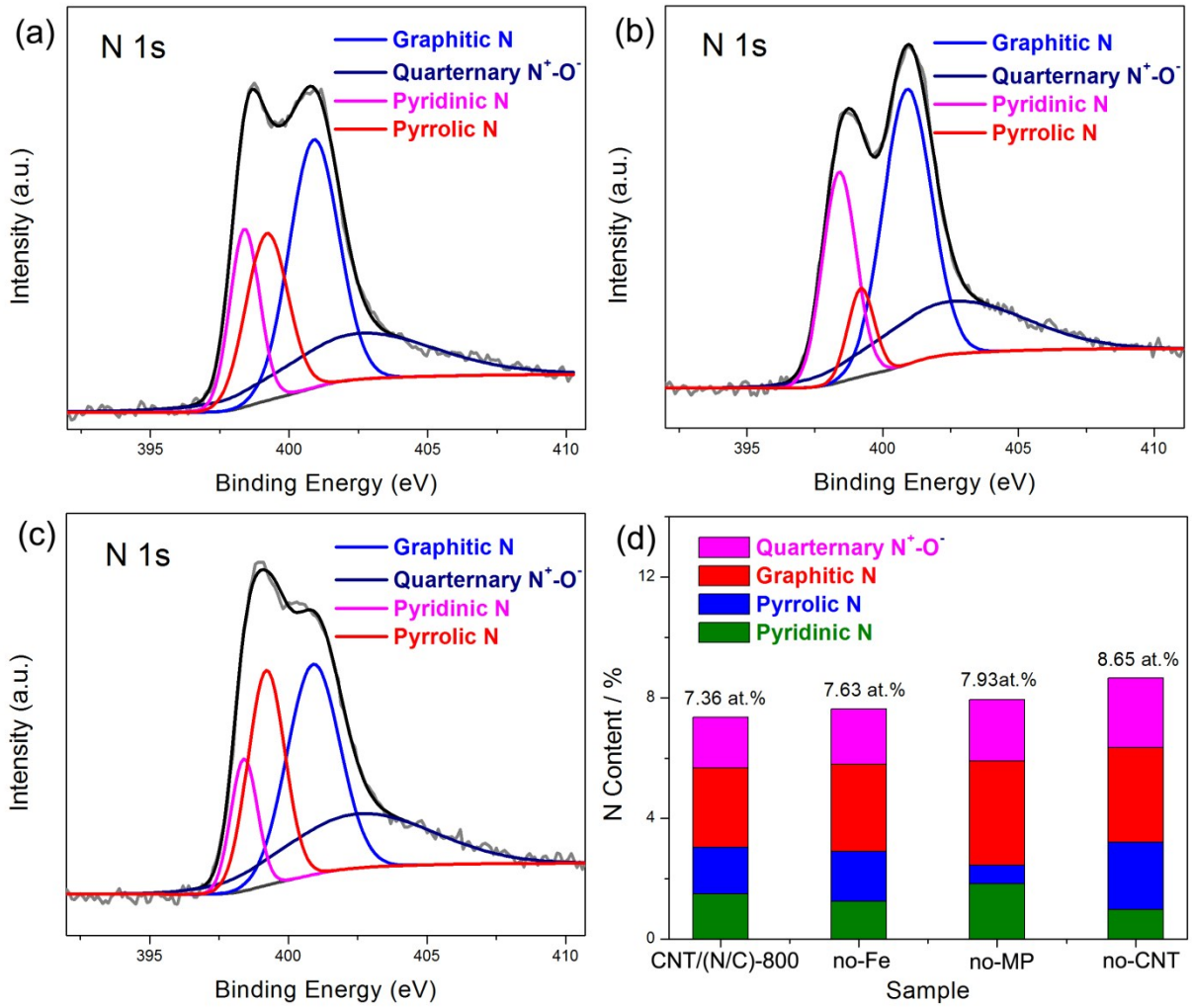

Figure S11. N 1s XPS spectra of the (a) no-Fe, (b) no-MP, and (c) no-CNT catalysts. (d)

Contents of pyridinic N, pyrrolic N, graphitic N, and quarternary N^{+}-O^{-} calculated in these samples.

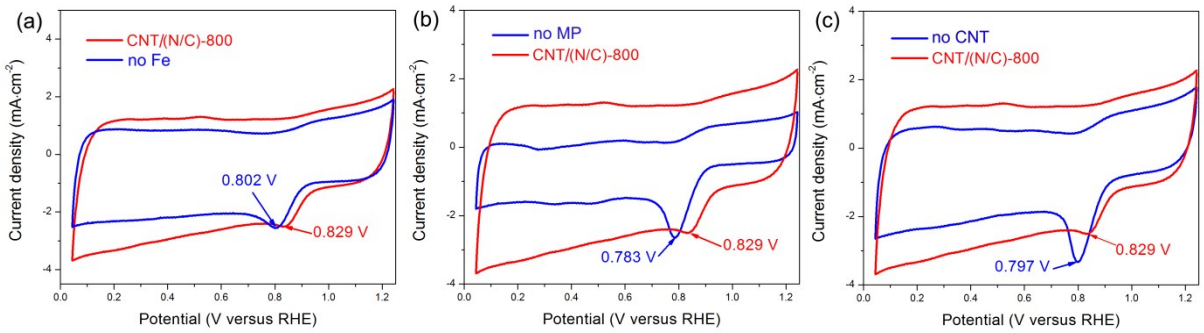

Figure S12. CV curves of the no-Fe, no-MP, no-CNT and CNT/(N-C)-800 catalysts measured in an O_2-saturated 0.1 M KOH solution at a scan rate of 50 mV/s.

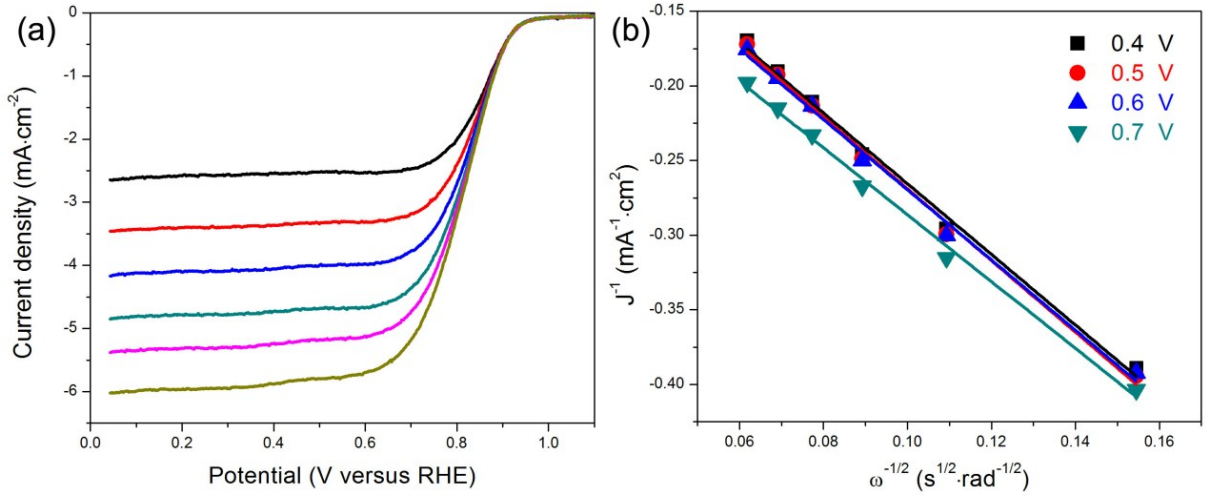

Figure S13. (a) RDE voltammograms of the no-Fe catalyst at different rotation rates and (b) the corresponding Koutecky–Levich plots at 0.4, 0.5, 0.6, and 0.7 V.

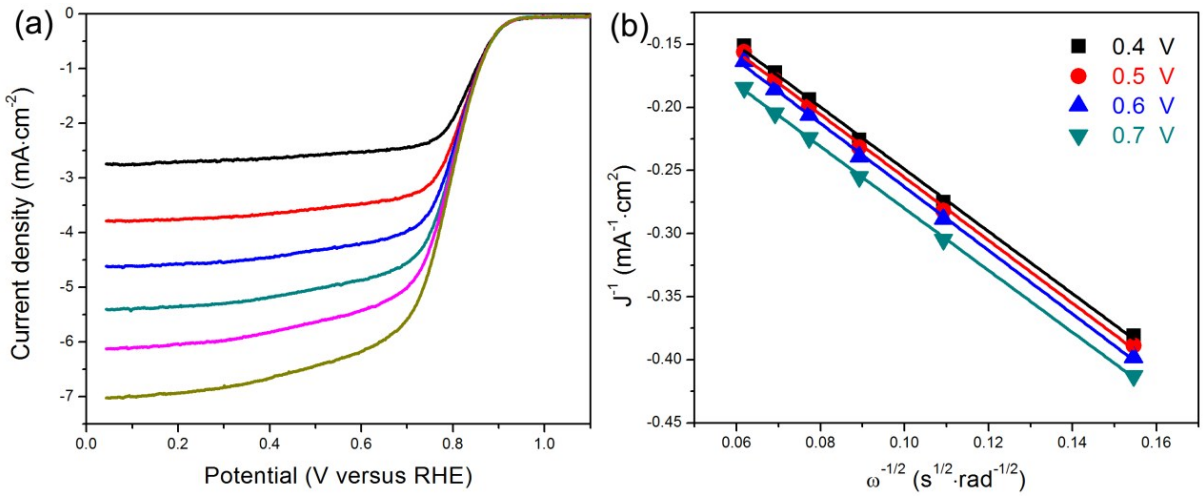

Figure S14. (a) RDE voltammograms of the no-MP catalyst at different rotatinon rates and (b) the corresponding Koutecky–Levich plots at 0.4, 0.5, 0.6, and 0.7 V.

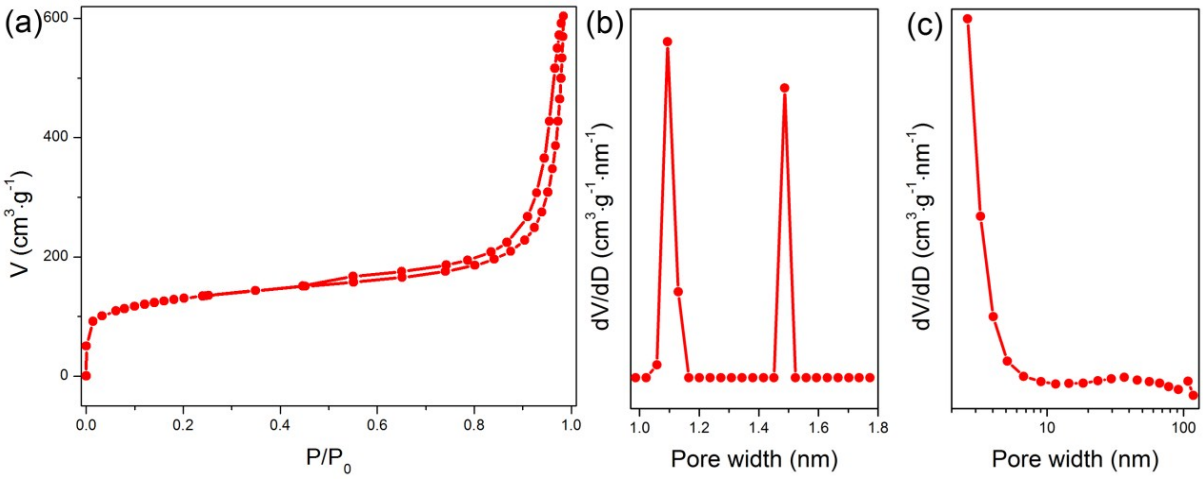

Figure S15. (a) N_2 adsorption/desorption isotherms of the no-MP catalyst. (b) and (c) are the corresponding pore size distribution curves.

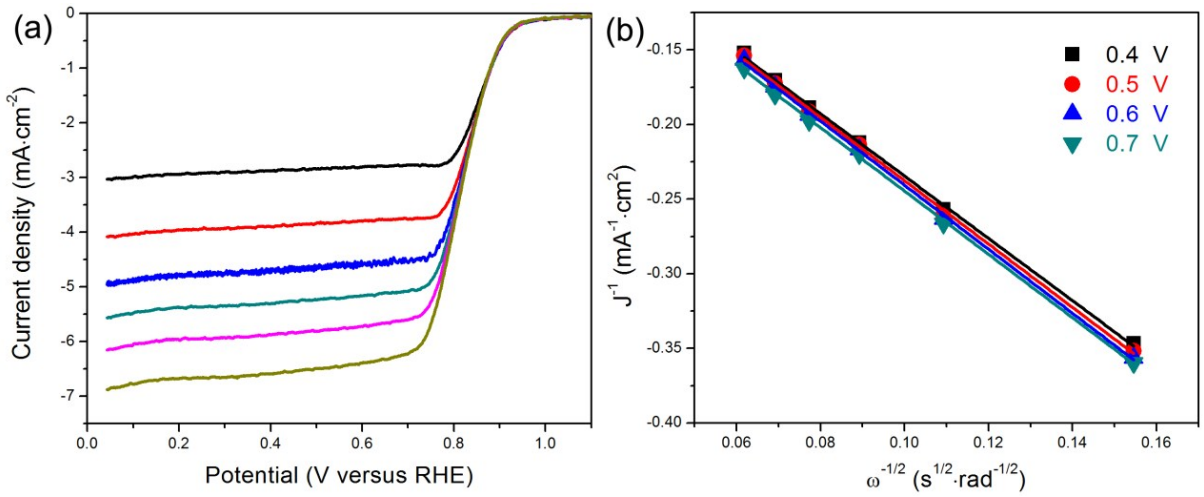

Figure S16. (a) RDE voltammograms of the no-CNT catalyst at different rotation rates and (b) the corresponding Koutecky–Levich plots at 0.4, 0.5, 0.6, and 0.7 V.

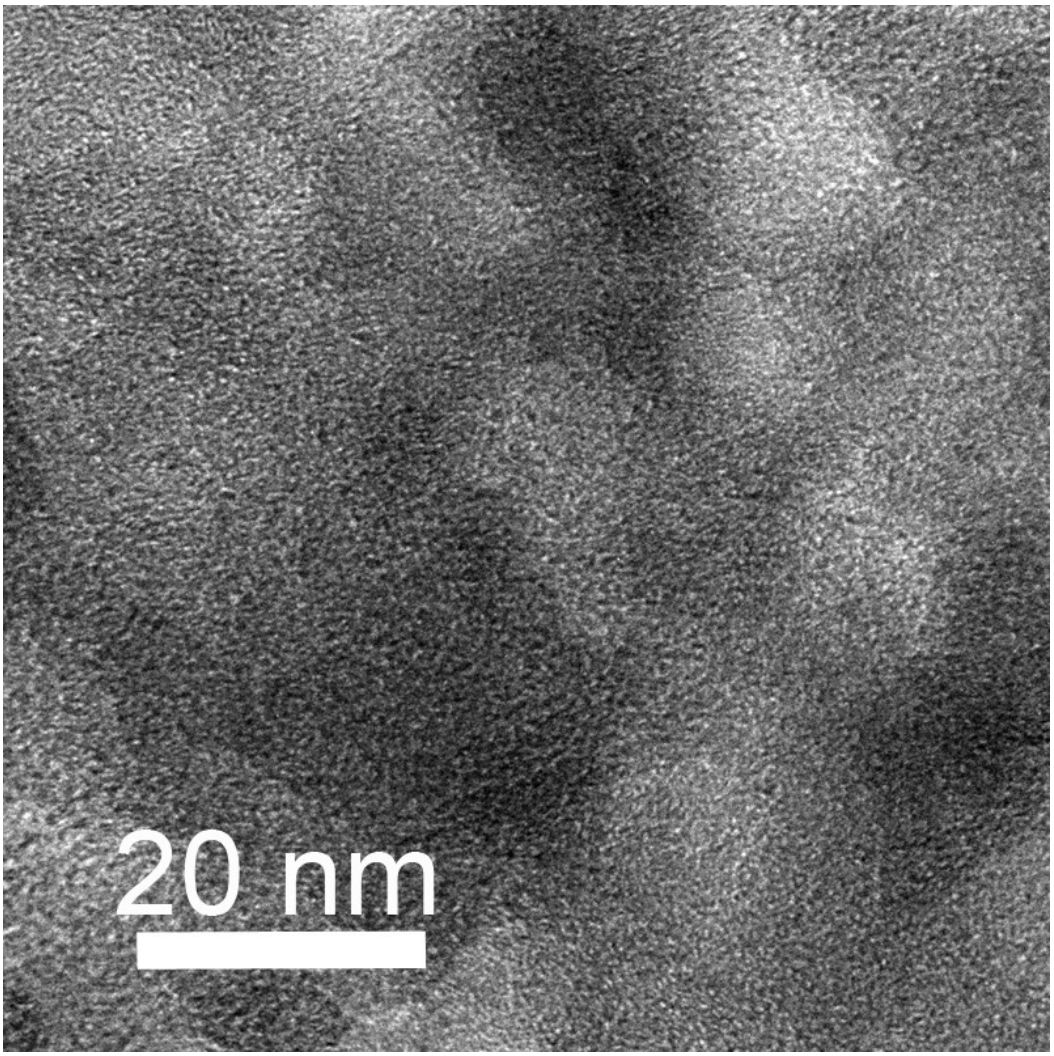

Figure S17. TEM image of the no-CNT catalyst.

Table S1. Elemental composition, specific surface area and electrocatalytic performance of the CNT/(N-C)-700, 800, 900 catalysts.

Sample	N at%	Fe at%	S_{BET} (m^2/g)	E_{onset}[a)] (mV)	$E_{1/2}$ (mV)	J (mA cm^{-2})	Loading (mg/cm^2)	Electron transfer number[b)] (n)
CNT/(N-C)-700	11.06	0.08	590	853	618	3.46	0.1	3.0
CNT/(N-C)-800	7.36	0.08	630	970	844	5.67	0.1	4.0
				1021	848	5.73	0.5	-
CNT/(N-C)-900	3.55	0.07	640	934	790	4.84	0.1	3.7
20 wt% Pt/C	-	-	-	962	818	5.63	0.1	4.0

[a)](In order to minimize the effect of residual currents on the potential value, the onset potential in this work has been defined as the potential required for generating an ORR current density of 0.1 mA cm^{-2} in a steady-state RDE experiment[8]); [b)](Electron transfer number was an averaged value calculated from the Koutecky–Levich equations at 0.4, 0.5, 0.6, and 0.7 V).

Table S2. A summary of the ORR catalytic activities of our catalysts and other transition metal/carbon catalysts reported recently (0.1 M KOH, 1600 rpm).

Material	Catalyst loading (mg/cm^2)	E_{onset} (mV, RHE)	E_{onset} (mV) versus Pt/C	J (mA cm^{-2})	Reference
Fe-N/C-800	0.1	923	-33	6.06	J. Am. Chem. Soc. 2014, 136, 11027-11033
Fe_xN/NGA	0.05	0.00 (vs Ag/AgCl)	Close to Pt/C	Close to Pt/C	Adv. Funct. Mater. 2014, 24, 2930-2937
N/Co-doped PCP//NRGO	0.714	970	-50	7.53	Adv. Funct. Mater. 2015, 25, 871-871

Co@Co3O4@C–CM	0.1	930	Close to Pt/C	<5	Energy Environ. Sci. 2015, 8, 568-576
Fe-N/C-800	0.079	980	+30	4.81	J. Am. Chem. Soc. 2015, 137, 5555-5562
CNT/(N-C)-800	**0.1**	**970**	**+8**	**5.67**	**This work**
	0.5	**1.021**	**+59**	**5.73**	

Table S3. The effect of Fe, mesopores, and CNTs on the ORR catalytic activities of the catalysts

Sample	N at%	Fe at%	S_{BET} (m^2/g)	E_{onset} (V)	$E_{1/2}$ (V)	J ($mA\ cm^{-2}$)	Electron transfer number (n)
CNT/(N-C)-800	7.36	0.08	630	0.970	0.844	5.67	4.0
no-Fe	7.63	~0	924	0.963	0.824	4.84	3.9
no-MP	7.93	0.10	514	0.924	0.814	5.55	3.7
no-CNT	8.65	0.25	716	0.967	0.828	5.43	4.0

References:

1. R. Liu, D. Wu, X. Feng and K. Müllen, *Angew. Chem. Int. Ed.*, 2010, **122**, 2619-2623.
2. J. Liang, X. Du, C. Gibson, X. W. Du and S. Z. Qiao, *Adv. Mater.*, 2013, **25**, 6226-6231.
3. H.-P. Cong, P. Wang, M. Gong and S.-H. Yu, *Nano Energy*, 2014, **3**, 55-63.
4. T.-N. Ye, L.-B. Lv, X.-H. Li, M. Xu and J.-S. Chen, *Angew. Chem. Int. Ed.*, 2014, **53**, 6905-6909.
5. S. Lee, M. Choun, Y. Ye, J. Lee, Y. Mun, E. Kang, J. Hwang, Y.-H. Lee, C.-H. Shin, S.-H. Moon, S.-K. Kim, E. Lee and J. Lee, *Angew. Chem. Int. Ed.*, 2015, **54**, 9230-9234.
6. J. Zhang, Z. Zhao, Z. Xia and L. Dai, *Nat. Nanotechnol.*, 2015, **10**, 444-452.
7. Y.-P. Zhu, Y. Liu, Y. Liu, T. Ren, G. Du, T. Chen and Z.-Y. Yuan, *J. Mater. Chem. A*, 2015, **3**, 11725-11729.
8. G. Wu, K. L. More, C. M. Johnston and P. Zelenay, *Science*, 2011, **332**, 443-447.